Atom Indonesia

Journal homepage: http://atomindonesia.brin.go.id

Source Identification Performance of Plastic Scintillator Ranging from 100–1300 keV: Assessment Through Monte Carlo Code and Experimental Validation

G. E. Putro[1,2*], M. R. Omar[1*], K. Kasmudin[2], H. L. Nuri[2], M. Pancoko[2], A. Jami[2], H. Subhiyah[2]

[1]*School of Physics, Universiti Sains Malaysia, 11800 USM, Penang, Malaysia*
[2]*Research Center for Nuclear Beam Analysis Technology, Research Organization for Nuclear Energy, National Research and Innovation Agency, Kawasan Sains dan Teknologi B. J. Habibie Serpong, Tangerang Selatan 15314, Banten, Indonesia*

ARTICLE INFO

Article history:
Received 14 December 2023
Received in revised form 24 October 2024
Accepted 29 October 2024

Keywords:

Gamma detector
Particle
Monte Carlo
Experimental
Efficiency
Resolution

ABSTRACT

Current plastic detectors need improvement in efficiency and accuracy to enhance reliability. Simulation offers a cost-effective approach to accelerate detector development, yet its effectiveness relies on the reliability of the simulations used. Therefore, validating these simulations is crucial to ensure they accurately reflect actual scenarios and yield reliable results. This study employs the Monte Carlo approach to estimate the performance and efficiency of a plastic detector exposed to radiation sources within the 100–1300 keV energy range. The plastic detector (50 mm x 3 mm) was simulated using MCNP with Gaussian Energy Broadening (GEB) correction applied to capture detector response. Simulated data were then compared against experimental measurements to validate the model. This work aims to confirm that simulation results align with empirical data, ensuring theoretical models accurately represent physical phenomena. The study highlights both the limitations and strengths of simulation codes, leading to more efficient research through validated models. Notably, an 8.04 % deviation was observed at 662 keV for ^{137}Cs, demonstrating a strong correlation between simulated and experimental results and confirming the model's accuracy and reliability.

INTRODUCTION

Intensive research on inorganic detectors like $LaBr_3$(Ce) has demonstrated their excellent light output and rapid decay time [1]. However, these detectors contend with issues, including hygroscopic properties that necessitate protective sealing [2] and relatively high manufacturing costs. In contrast, plastic scintillators offer numerous advantages: they have lower density, a fast response time of 4 ns [3], and cost-effectiveness, and they can be readily shaped through extrusion, injection molding, or casting. Recent advancements have focused on incorporating high-Z compounds such as triphenyl bismuth ($BiPh_3$) to enhance photon peak detection and address issues like dominant Compton scattering [4], thus, broadening their applications in both scientific research and industrial settings.

The Monte Carlo (MC) method, a computational technique based on stochastic processes, is widely utilized across various radiation-related applications. It is essential in fields such as radiological safety, nuclear facility design, radiation protection simulation, and computational modeling of detectors, where it aids in managing potentially hazardous radiation levels. The method's stochastic nature arises from its use of statistical sampling from probability distributions across spatial domains, allowing it to accurately model photon behavior in specific environments [5]. Moreover, the Monte Carlo technique has become indispensable for nuclear transport simulations where direct physical measurements are impractical or challenging. It also significantly supports data collection for the development and training of

*Corresponding author.
E-mail address: guntur.eko.putro@brin.go.id, rabieomar@usm.my
DOI: https://doi.org/10.55981/aij.2025.1401

machine learning models in a range of nuclear applications.

In this study, we utilized the Monte Carlo N-Particle (MCNP) code was employed as a computational tool to evaluate the performance of a plastic scintillator. This implementation enhances our capability to assess the detector's response characteristics. While the MCNP code does not fully simulate the scintillation process, it effectively calculates energy deposition across simulated material. Additionally, as the photomultiplier tube (PMT) captures particle interactions within the scintillator's active volume, the simulation results provide a comprehensive representation of the scintillator's response [6]. The strong correlation between these computational results and experimental data highlights the reliability and accuracy of the simulation approach used.

The MCNP code utilizes a versatile Monte Carlo nuclear transport algorithm designed to simulate a wide range of particle types, including electrons, photons, and neutrons. Rather than directly solving the Boltzmann transport equation, the code models the trajectories of individual particles, capturing detailed data related to their characteristic behaviors [7]. It effectively simulates the probabilistic particle interactions with materials sequentially, employing statistically derived probability distributions and pseudo-random number generation. This comprehensive approach tracks particles from their source through various material interactions until reaching a predefined energy cutoff, accounting for factors such as escape, physical boundaries, and absorption [8].

To accurately calculate results at each stage of a particle's trajectory, probability distributions are carefully sampled from detailed transport records. In parallel, relevant quantities are efficiently computed using approximations to rigorously assess the analytical accuracy of the outcomes. This sophisticated code is adept at modeling complex photon interactions, including the Bremsstrahlung effect, fluorescence, Thomson and Compton scattering, and pair production. Furthermore, the program is uniquely capable of predicting discrete particle pathways while simultaneously modeling the stochastic interactions between particles and materials [9].

Recent studies utilizing Monte Carlo simulations have significantly advanced plastic scintillation research, particularly for applications requiring precise radiation detection. One study simulated the pulse shapes of plastic scintillators using Geant4, highlighting the potential of Pulse Shape Discrimination (PSD)-capable scintillators in distinguishing between neutron and gamma radiation. This research emphasizes the importance of integrating simulation data with photomultiplier tube responses to optimize detector performance [10]. Another study evaluated a multi-array plastic scintillator system for radiation portal monitors, crucial for detecting illegal radionuclide transport. By employing Monte Carlo simulations, researchers optimized the geometric configuration of the scintillator array, improving detection efficiency and energy resolution. These design enhancements notably increased the accuracy of radionuclide identification in security applications [11]. A third study focused on optimizing small animal gamma-optical cameras, investigating various scintillator thicknesses and septa materials using Monte Carlo simulations. Thicker detectors enhanced sensitivity at the expense of spatial resolution while black tape for septa improved resolution. These findings contribute to refining gamma camera designs for improved diagnostic imaging in veterinary applications [12].

Despite advancements in simulation methods, it is crucial to recognize that the quantity of photons emitted during photomultiplier discharge can vary significantly. This variability is a key factor influencing the scintillator's high resolution and sensitivity. Consequently, accurately accounting for this variation in energy response during simulations is essential, with experimental data playing an essential role in ensuring accuracy [13]. The integration of precise models with empirical evidence from experiments provides a more comprehensive understanding of the scintillator's performance, thereby improving the reliability of its response in practical applications.

Current plastic detectors, widely used in various applications, face significant challenges related to their efficiency and accuracy. Addressing these challenges necessitates substantial enhancements to improve their reliability and performance. The integration of advanced simulation techniques provides a cost-effective solution to accelerate detector development and reduce overall costs. However, the effectiveness of these simulations depends on their accuracy and the well they replicate actual scenarios. Therefore, validating these simulation models is crucial to ensure they not only reflect actual conditions accurately but also produce consistent results. This validation process is essential for advancing the technology and ensuring that simulations remain a reliable tool for optimizing plastic detectors.

This work aims to evaluate the differences between simulation results and actual experimental data by validating the Monte Carlo simulation outcomes, particularly focusing on the performance of the MCNP code with Gaussian Energy Broadening (GEB) adjustments. To achieve this,

key performance metrics of the detector, including efficiency, resolution, and full-width half maximum (FWHM), are analyzed to assess the accuracy and effectiveness of the simulation code. The expected outcomes of this research include the development of a validated and reliable Monte Carlo simulation model that accurately represents actual radiation detection scenarios, specifically for plastic scintillators with GEB adjustments. This validation will enhance the accuracy of simulations in predicting detector performance and provide valuable insights into the limitations and strengths of simulation codes.

In addition to validation, this study aims to investigate the impact of GEB modifications on simulation outcomes. The research will assess how GEB adjustments influence simulation accuracy, utilizing the Monte Carlo technique as a primary method. Additionally, the potential correlation between GEB modifications and simulation results will be examined to enhance understanding of GEB's effects on outcomes within the targeted energy range. By integrating Monte Carlo simulations, GEB adjustment, and experimental validation, this research seeks to optimize simulation accuracy and efficiency. Validated models can significantly reduce the need for extensive and costly experimental trials.

METHODOLOGY

The study employs Monte Carlo computational modeling to analyze the response of plastic scintillators, with experimental measurements, establishing a correlation between energy and resolution for evaluating simulated spectra. The measured results were then compared with MCNP model estimates to validate the experimental findings for the scintillator model. Photon source activity was determined by placing a detector at a defined distance from the source along the detector's axial position, with similar geometries subsequently simulated in MCNP. Standardized sources with representative energy levels, as detailed in Table 1, were used for consistency across both experimental and simulated conditions.

Table 1. Photon source characteristics.

Isotope (Source)	Energy (keV)	Probability (%)	Compton Peak (keV)
^{60}Co	1173/1332	99.87 ± 0.06	1040
^{137}Cs	662	84.6 ± 0.5	477

Note: Probability (%): the likelihood of a photon emitting at the specified energy level from a source. Compton Peak (keV): the highest energy observed after undergoing Compton scattering.

Experimental work

The scintillator was experimentally characterized using conventional gamma-spectrometer tools, with the experimental configuration illustrated schematically in Fig. 1 [14]. The polystyrene scintillator ($[C_8H_8]_n$) manufactured by Epic Crystal, was designed as a cylinder to align with the photomultiplier tube (PMT) dimensions, measuring 50 mm in diameter, 3 mm in thickness, and a density of 1.05 g/cm^3. This research utilized ^{137}Cs and ^{60}Co as radiation sources, both commonly used in medical physics research and treatments. The detector setup, implemented at the Research Organisation for Nuclear Energy (ORTN BRIN), included an R878-800V Hamamatsu photomultiplier (PMT) paired with a Gamma Spectacular multichannel analyzer for precise measurement.

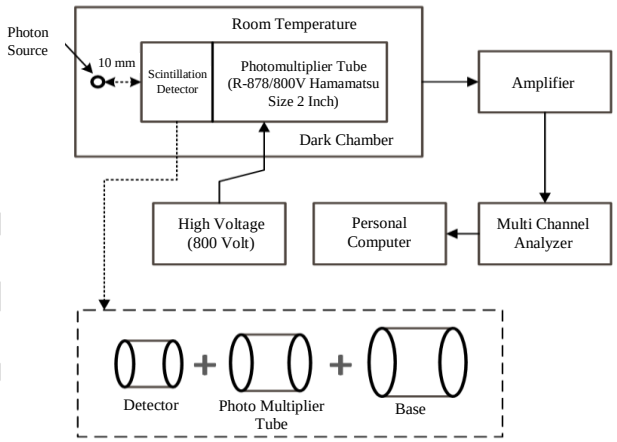

Fig. 1. Illustration of experimental configuration.

A delay amplifier (DA) was connected to the end of the scintillator to address baseline instability, which can adversely affect measurement accuracy and the precision of gamma radiation energy analysis. This configuration is expected to improve both the accuracy and reliability of signal acquisition for energy spectrum measurements in practical applications. The bipolar output of the amplifier was connected to a multichannel analyzer (MCA) from Bee Research, facilitating the acquisition of the energy spectrum associated with the photon sources.

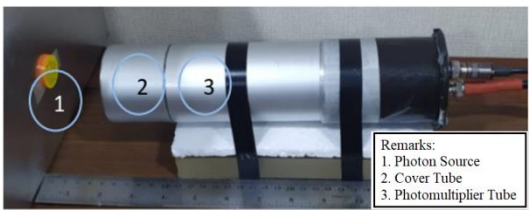

Fig. 2. Assembly of measurement device.

Figure 2 depicts the detector setup, with the scintillator mounted in the front of the

photomultiplier tube (labeled No. 3 in the figure) using optical grease, housed within a reflector, and enclosed in an aluminum cover tube (No. 2). The detector was positioned approximately 10 millimeters from the photon source (No. 1) to maintain a consistent measurement distance. The energy spectrum is acquired using the Theremino program on a personal computer for 300 seconds, which helps minimize inaccuracies or errors around the peak, targeted to be within 5 %. The detector, shaped like a cylinder with a diameter of 50 mm, is shown in Fig. 3, where the process of obtaining the energy spectrum is illustrated.

Fig. 3. Prepared detector for spectrum measurements.

Monte carlo method

The Monte Carlo technique is a stochastic method widely used to address radiation transport challenges in areas such as radiation detection, dosimetry, and other related field. Recognized for its accuracy in analyzing detector performance, the Monte Carlo method has become an increasingly effective alternative to traditional methods, particularly with the advancement in computational science. This technique provides significant advantages, including the ability to simulate laboratory experiments without requiring radioactive sources and delivering precise computational results. The method relies on stochastic processes, simulating particle movement within a defined system, using statistically derived data from relevant probability density functions. A key aspect of these simulations is the "history" of individual particles, which encompasses their trajectory from the point of origin to their endpoint, either by absorption or escape from the system's boundary [15], which is critical in these simulations. The efficacy accuracy of Monte Carlo simulations, however, is strongly influenced by the accurate representation of the detector's geometry and composition.

The response of a detector is characterized by the variation in the pulse height spectrum resulting from the interaction of monoenergetic particle radiation with the scintillator, influenced by particle cross-section interactions within the scintillator material. During both measurement and simulation phases, the detector responses are broadened by several factors including variability in light output, the statistical behavior of photon generation within the detector, fluctuations in collection efficiency, variations in the number of particles generated, intrinsic scintillator fluctuations, and noise from the electronic device [16]. An accurate definition of the response characteristic near the observed spectra requires discrete and cumulative computations of these physical effects, a process that poses significant challenges.

The energy deposition distribution of simulated particles within the active volume of the investigated detector was evaluated using pulse height calculation (F8 tally) via MCNP. This process quantifies the energy absorbed by local particles as they interact with surrounding atoms during each unique initiating history. To ensure statistically reliable results across the energy spectrum, simulations were conducted with a historical count of 20 million particles, achieving an uncertainty of 3 % or less in the Compton region and other relevant areas [17]. The pulse height output was recorded using energy bins with a width of 1 keV each. Figure 4 illustrates the geometry of the plastic detector used in the simulation.

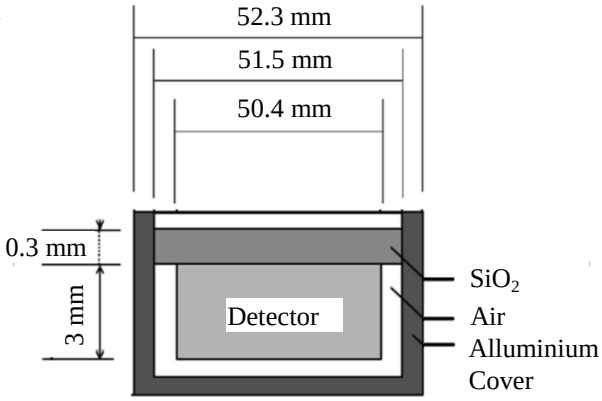

Fig. 4. Plastic detector geometry used in this study.

Energy resolution

Detector resolution indicates the ability of a detector to differentiate between particles that have nearly identical energies. Typically, the inherent resolution inherent in the detector material surpasses what is achievable in practical scenarios. This resolution, denoted as R, is quantified by the full-width half-maximum (FWHM) at the peak of the energy distribution (E_0) as presented in Eq. (1).

$$R = \frac{FWHM}{E_0} \quad (1)$$

The Full-Width Half-Maximum (FWHM), is calculated by measuring the width of an energy spectrum peak at its half-maximum height. This width is defined as the distance between two points on the peak where the intensity is equal to half of the peak's maximum height, as depicted in Fig. 5. FWHM is a key metric for evaluating the separation between energy peaks in a spectrum, essential for assessing a detector's capability to distinguish and accurately measure the energy of different photons or particles interacting with the detector [18].

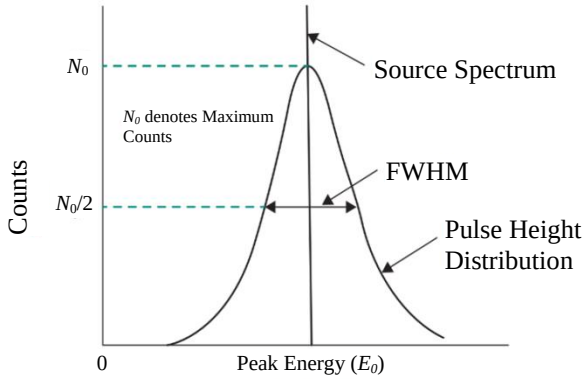

Fig. 5. FWHM determination technique from pulse height distribution.

The resolution of the energy peak in a scintillator connected to a Photomultiplier Tube (PMT) is influenced by both the intrinsic properties of the scintillator and the effects of the PMT. The laser contributes to the broadening effect due to a final number of particles in the output signal. Experimental energy distribution typically exhibits a Gaussian profile across the relevant energy regions. However, while MCNP (Monte Carlo N-Particle) simulation software does not directly simulate the physical processes responsible for spectrum broadening, it accounts for detector resolution by employing a fitting function specified in the input data [19].

Multiple simulation runs were conducted to determine the resolution of the detector, taking into account the materials of the housing, detector, and PMT used in the current research. To enhance the accuracy of the MCNP simulation outcomes, it is essential to incorporate energy resolution adjustments using the Gaussian Broadening special card feature (GEB). This process involves applying an F8 tally combined with the GEB FT8 special command in MCNP to accurately determine the peak of the FWHM. To implement these corrections, several coefficients derived from the energy curve are integrated into the formula specified in MCNP. This formula, based on Gaussian principles, adjusts the energy spectrum to account for detector resolution. By employing Gaussian distribution sampling, the calculated energy spectrum is effectively broadened as expressed in Eq. (2).

$$f(E) = Ce^{-\left(\frac{2\sqrt{\ln 2}\,(E-E_0)}{FWHM}\right)^2} \quad (2)$$

Where E_0 means the tally's unbroadened energy, E means broadened energy, and C represents a certain constant. This function enables the application of Gaussian broadening, effectively simulating the physical behavior of gamma scintillators. The Gaussian broadening technique, available in MCNP as a special technique for F8 tallies, applies the formula provided in Eq. (3).

$$FWHM = \alpha + \beta\sqrt{E + \delta E^2} \quad (3)$$

Where α, β, and δ defined in MCNP, while E represents the particle energy [9]. These constants characterize various aspects of the energy distribution's shape and scale and are derived from fitting experimental data to the model, as shown in Fig. 11(a) using Eq. (3). Specifically, the values obtained from these fittings are 0.0064, 0.0986, and 0.9980, respectively.

Efficiency calculation

The formal definition of absolute efficiency for particle detectors is expressed as a proportion, as shown in Eq. (4).

$$\varepsilon = \frac{Nc}{Ne} \quad (4)$$

where *Nc* represents the number of particles captured by the detector, and *Ne* represents the total number of emitted particles by the source. This efficiency is affected mainly by the intrinsic characteristics of the detector and, to a lesser extent, by counting geometry. Key factors include the distance between the source and detector, the energy of particles, and the probability of particle emission [20].

To validate the computational simulation of the scintillator, experimental results measuring the efficiency of specific sources, as listed in Table 1, were compared to the simulation-generated values, both obtained under similar experimental conditions. The sources were positioned at a fixed distance of 10 mm from the detector, aligned along the scintillator's longitudinal direction, to minimize the cumulative effects, enhance tally statistics, and approximate the

particle emitter as a single point in space. The setup also defined a 300-second calculation interval and maintained a consistent source-to-detector distance to ensure that associated counting errors remained below 5 %. Furthermore, to accurately assess the performance of the scintillator, considerations were made regarding the dimensions of the scintillator and the materials surrounding it, particularly for particles with energy under 300 keV [13].

The scintillator efficiency with given energy can be determined using Eq. (5) [21].

$$\varepsilon = \frac{C}{A.P.t} \quad (5)$$

Where C refers to the observed net counts, A is the activity of particle source during measurements (in becquerel), t denotes the measurement interval (in seconds), and P refers to the probability of photon emission. In application, the counts (C) for a specific peak can be calculated by manually specifying a region near the observed peak. The program then determines the peak position and its area after subtracting the background count.

Gaussian Energy Broadening (GEB)

The GEB describes the widening of the energy distribution due to interactions of particles within the detector. This broadening results from various factors, such as variations in light production, optical scattering, and electronic noise. As photons travel through the detector, they undergo multiple collisions, losing energy with each interaction. However, the number of collisions and the amount of energy lost in each one are not uniform, leading to energy spread, or energy straggling. While energy straggling is negligible when determining the total energy of charged particles, it becomes significant in transmission studies, where the particle exits the detector after depositing only a fraction of its energy.

In the classical approach, the variance of energy straggling is determined as shown in Eq. (6).

$$\sigma_E^2 = 4\pi r_0^2 (mc^2)^2 Z_1^2 Z_2 N \Delta x \quad (6)$$

Where $Z_{1,2}$ represents the charge of the incoming particle, Z signifies the atomic number of the material, Δx refers to the material's thickness, N stands for the atom count per cubic meter, and r_0 Indicates the radius of the particle.

To estimate energy straggling, a vacuum chamber, a particle source, detector material, and a movable absorber are used to ensure that no energy is lost as particles travel from the source to the detector. The straggling width is calculated using Eq. (7).

$$\Gamma_s = \sqrt{\Gamma^2 - \Gamma_d^2} \quad (7)$$

To determine the width Γ_d, the energy spectrum of the particles is recorded without the absorber in place. The width Γ is then measured by analyzing the spectrum after the absorber is introduced. By using absorbers of varying thicknesses, the dimension Γs can be analyzed along the particle's trajectory (Δx). Several studies have been conducted for this purpose, particularly with alpha radiation. For very thin absorbers, the experimental data agrees with theoretical predictions, but for thicker absorbers, the theoretical model fails to accurately predict the observed width [22].

Another factor contributing to GEB is the randomness inherent in scintillation, where the emission of light photons due to particle interactions varies statistically. Additionally, optical flaws and material impurities within the scintillator can further cause the energy spectrum to widen. Furthermore, electronic interference during the signal processing phase may amplify the effects of GEB, expanding the detector's energy response.

This expansion of the energy spectrum due to GEB greatly affects the detector's performance. It can reduce the precision of energy measurements and hinder the detector's ability to accurately measure the energies of particles. Therefore, applying appropriate correction methods is essential to mitigate the impact of GEB and to ensure accurate radiation data when using scintillation detectors [23].

Pulse-Height distribution

The pulse-height tally method in MCNP fundamentally differs from the conventional tallying techniques used in the program. While other tallies typically compute macroscopic quantities like flux by accumulating numerous small-scale events, the pulse-height tally operates on a distinct principle. It specifically records the energy deposited within a specified cell by individual particles and its resulting secondary interactions. In essence, conventional tallies focus on calculating expected values of large-scale variables, often neglecting individual microscopic interactions. In contrast, the pulse-height tally requires a more detailed and realistic simulation of microscopic events to achieve accurate data representation.

The pulse-height tally is particularly advantageous for counting photons and electrons, as implemented using the F8 card. The accuracy of the results is strongly influenced by the thickness of the cells involved: ensuring that these cells have adequate thickness is important to minimize errors caused by fluctuations in energy loss rates. However, applying F8 cards to photonuclear cases can create significant challenges, often resulting in inaccurate data, despite their intended purpose of identifying potential issues in the model that may influence the resulting quality.

Tracking the outcomes of F8 card calculations is a key step at the end of each simulation sequence. When variance reduction methods are not applied, the process becomes relatively straight forward, facilitating accurate data collection. The calculation for the total energy deposited (T) is outlined in Eq. (8).

$$T = \sum_{i=1}^{K} E_i - \sum_{j=1}^{L} D_j \quad (8)$$

Where K and L indicate the number of particle entries and exits for specific cells, respectively. Meanwhile, E_i and D_j denote the energies of the i^{th} and j^{th} particles as they enter and leave the cells [9].

Feasibility analysis: PPV scintillator

Utilizing the Monte Carlo simulation methodology, the detector responses of Poly(para-phenylene vinylene) (PPV) scintillators were analyzed and compared with those of Polystyrene (PS) to assess their performance and viability as scintillators. PPV, represented by its repeating chemical unit $(C_8H_6)_n$, exhibited a density of 1.1–1.2 g/cm³, a refractive index of ~1.8, and an optical transparency exceeding 90 % in the visible spectrum [24,25]. The detector models for PPV were developed to replicate those of PS, maintaining consistency in geometric configurations, radiation sources, and simulation parameters. This modeling included detailed specifications of the radiation detection setup, instrumentation, simulation procedures, and other relevant physical parameters. Both scintillators were subjected to identical simulation conditions to ensure a direct and reliable comparison of their performance. The feasibility of PPV as a scintillator, in comparison to PS, was evaluated based on several criteria: performance metrics derived from pulse height distributions, cost-effectiveness of production, and chemical stability.

RESULTS AND DISCUSSION

The results from Monte Carlo (MC) simulations and the experimentally detected photon spectrum from a plastic scintillator exposed to radiation sources are compared, as depicted in Figs. 6(a) and 6(b). This comparison is critical for evaluating detection performance, particularly emphasizing the Compton peak for ^{137}Cs appears around 490 keV, while for ^{60}Co around 1100 keV. These findings align well with previous research [23,26,27], indicating an acceptable agreement between the experimental and simulated spectra. For ^{137}Cs, both the experimental and simulated spectra reveal the presence of the Barium (Ba) K-shell X-ray peak at approximately 32 keV. This peak results from the decay of ^{137}Cs into its short-lived metastable product, ^{137m}Ba, through beta decay. The decay involves the emission of particles, including beta particles, showcasing a critical aspect of nuclear decay mechanisms.

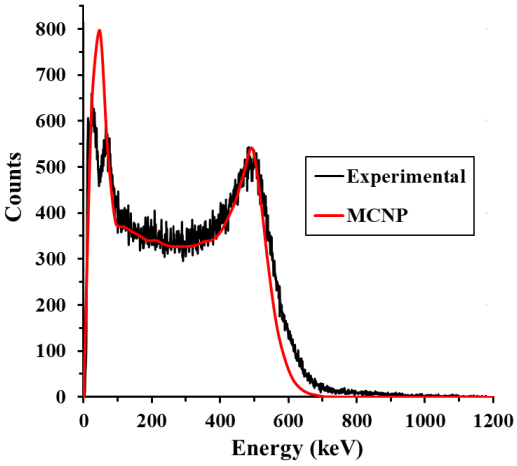

(a)

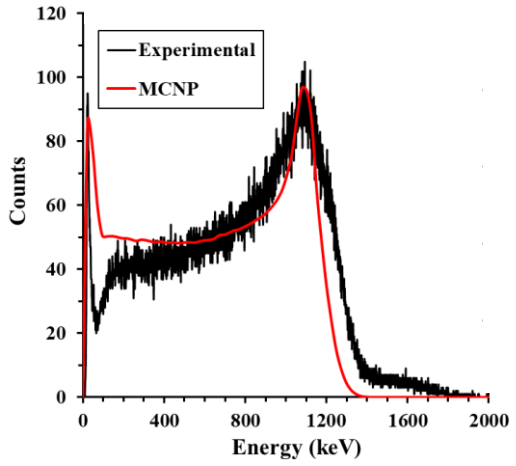

(b)

Fig. 6. Pulse height profile for simulation and experimental results: (a) ^{137}Cs; (b) ^{60}Co.

The generation of gamma particles through an excitation process, similar to the emission of infrared or visible photons, results in the decay of material into the stable state of Barium. This transition is characterized by distinctive spectrum properties associated with Barium K-shell X-ray emissions. However, a systematic discrepancy has been observed in the intensity of the Barium X-ray peak, where the observed spectrum consistently shows lower values than those predicted by Monte Carlo models. This discrepancy likely stems from the scattering of gamma particles by nearby materials and surroundings, which can alter the detected emissions.

The performance of detectors, particularly at lower energy levels, plays a critical role in accurately capturing emissions. Physical detectors frequently exhibit uneven responses, resulting in incomplete detection of radiation that passes through. This issue is especially pronounced for X-rays, which are prone to being absorbed or deflected before reaching the detection surface. In practical application, low-energy photons, such as those emitted from Barium X-ray sources, are susceptible to absorption or scattering by detector components and adjacent materials. These interactions result in a noticeable reduction in the observed intensity of the Barium peak compared to the simulations, with additional intensity losses typically occurring within the detector environment due to these interactions [28].

The study's findings highlight the need for improved simulation accuracy and advanced detector design to better account for scattering effects and interactions, which are critical for precise radiation measurement. This includes the development of new scintillator materials and detector configurations capable of more effectively capturing low-energy photons, thereby mitigating their susceptibility to absorption and scattering. Future research should focus on refining simulation models and innovating detector materials and designs to optimize the accuracy of radiation interaction measurement and overall detection performance.

Figures 7(a) and 7(b) present a cross-validation curve comparing the results of the MCNP simulation and experimental measurements. The diagonal line represents the identity line, indicating good agreement between simulation and experimental results. Data points closer to this line demonstrate a strong correlation between the two datasets. Most of the data points for ^{137}Cs cluster around the line, suggesting that the MCNP simulation results are generally consistent with the experimental measurements obtained using the plastic scintillator gamma radiation detector.

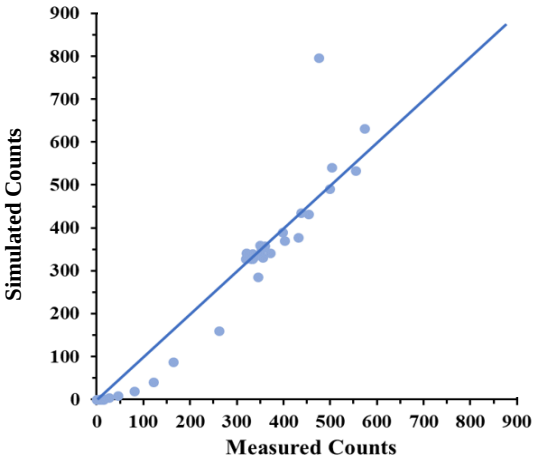

(a)

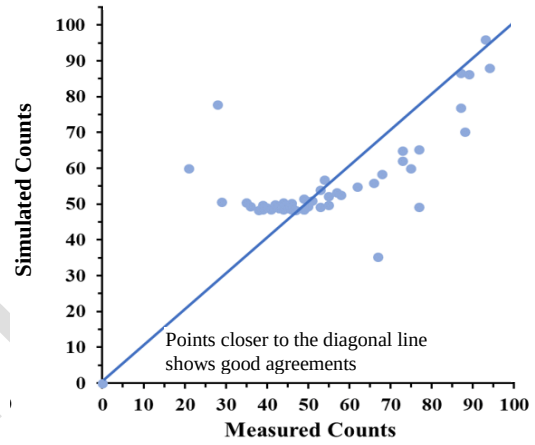

(b)

Fig. 7. Cross-validation curve for simulation and experimental results: (a) ^{137}Cs; (b) ^{60}Co.

For the ^{60}Co results, several data points are clustered around the mid-range of measured counts. While most of these points are relatively close to the identity line, indicating moderate agreement, some deviations are observed, particularly at higher count levels where data points fall further from the line. These deviations may be attributed to the Gamma-ray scattering phenomenon, which affects the measurement using plastic detectors. Gamma-ray scattering refers to the deflection of gamma rays as they interact with surrounding substances and the environment. When gamma rays collide with atoms in nearby materials, their trajectories change, potentially increasing or decreasing the counts detected by the scintillator [29].

Future work should focus on enhancing simulation models to more accurately predict the effects of environmental interactions, such as gamma scattering, on detection accuracy. This could involve integrating more complex physical models into simulations that account for the diverse gamma rays interacting with various materials. Additionally,

advancing materials and designing detectors capable of minimizing the impact of scattering could significantly improve the accuracy and reliability of gamma radiation detection systems.

To study the effect of the GEB feature in MCNP, pulse height spectra were calculated under two conditions: with and without GEB, using ^{137}Cs and ^{60}Co sources, as shown in Fig. 8. This comparison highlights the significance of using the GEB feature. The results indicate that simulations without the GEB produce values for the Compton peak that are 19 % and 34 % higher for ^{137}Cs and ^{60}Co, respectively, compared to simulations with GEB. These findings suggest that the GEB feature has a substantial impact on the pulse height spectra.

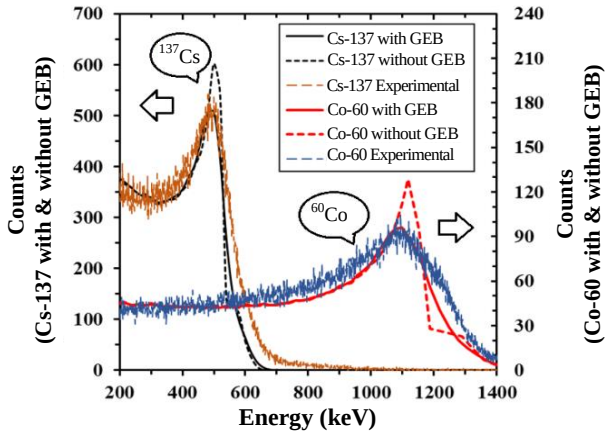

Fig. 8. Pulse height spectrum obtained from simulation with and without GEB treatment.

The differences can be attributed to the fact that simulations without GEB fail to account for the broadening of energy peaks caused by factors, including electronic noise and energy straggling, which are common in actual applications. By neglecting these factos, simulation yield higher value, as they do not accurately reflect realistic condition. Th inclusion of GEB enhances the reliablity of simulations by integrating effects found in practical applications [19,22]. Future research should focus on refining simulation parameters and expanding the application of GEB to other isotopes and detection scenarios. This could further improve diagnostic capabilities and advance research tools in nuclear physics and medical imaging.

Scintillator efficiency

The Monte Carlo simulations were utilized to assess the efficiency of the detector, with the resulting values compared to experimental results to verify the accuracy of the simulation. The calculated margins of error, which considered variations in counts, radionuclide activity, and emission probabilities, consistently remained below 5 %.

In Fig. 9, the measured efficiency derived from experimental data and the simulated efficiency curves are presented as a function of energy. Simulations were extended to energies not directly measured, providing a curve that aligns well with actual measurements within the energy range of 100 to 1300 keV. Figure 9 illustrates both similar measured energy and the related simulated data to support comparative analysis. Both simulated and experimental results demonstrated satisfactory agreement, with the relative difference (RD) of 8.04 % observed for ^{137}Cs in the energy of 662 keV, as shown in Table 2.

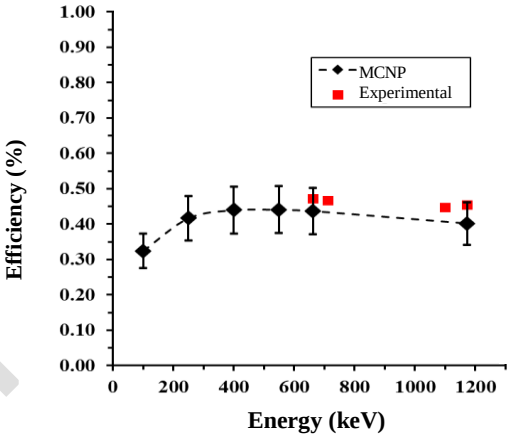

Fig. 9. Efficiency curve of plastic detector based on experimental and simulation results.

Table 2. Comparison of simulated and experimental.

Variable	Source (Energy)	Simulation	Experimental	% RD
Efficiency (%)	^{137}Cs (662 keV)	0.437	0.472	8.04
	^{60}Co (1173 keV)	0.402	0.455	13.12
FWHM (keV)	^{137}Cs (662 keV)	69.30	65.67	5.24
	^{60}Co (1173 keV)	126.77	115.44	8.94
Resolution	^{137}Cs (662 keV)	0.140	0.132	5.79
	^{60}Co (1173 keV)	0.117	0.106	10.11

Notes: %RD represents the relative difference between simulation results and experimental data.

The graph shows an increasing efficiency curve, beginning with a rise in detection capabilities as the energy escalates from 100 keV, peaking between 300-400 keV before gradually declining. This peak indicates the most effective range for detecting efficiency with the plastic scintillator material used in this research. When compared to the experimental data, the results from MCNP simulations align well with the actual measurement of around 600 keV, indicating the simulation's accuracy in simulating true detector

responses at lower energies. However, at higher energy levels, the sparse and scattered experimental data points indicate growing deviations from the simulated results.

The discrepancies observed between simulated and actual results might be due to scattering effects associated with high-energy photons. While detectors are primarily designed to capture photons, scattering can affect the accuracy of these measurements. When photons scatter, they may fail to deposit all their energy at the point of impact or could even escape the detection area entirely. Consequently, the recorded energy readings, which are either underestimated or varied, may not accurately reflect the true energy of the incoming particles [30]. Future research should focus on improving simulation techniques to better account for scattering phenomena, potentially incorporating advanced computational models. This could lead to the development of more precise detectors, enhancing applications in fields requiring accurate radiation measurements, such as medical imaging and environmental monitoring.

To provide a more comprehensive comparison of the efficiency in this research with detector responses in previous literature, we presented the simulated and experimental NaI(Tl) efficiency data obtained from Salgado et al. [31], as depicted in Fig. 10, which showed a good level of alignment.

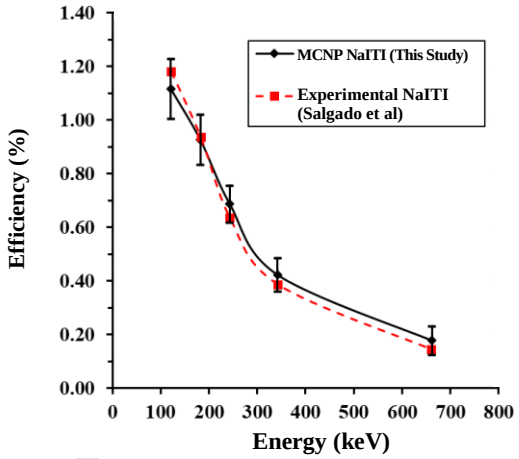

Fig. 10. Comparison of detector efficiency (%) of NaITl detector based on experimental data by Salgado et al. [31] and simulation (this study) results.

Figure 9 clearly illustrates the efficiency trends of NaI(Tl) scintillators across a range of energies. Both the Monte Carlo simulations conducted in this work and the actual data collected by Salgado et al. demonstrate a decline in detector efficiency as the energy level rises. This observed trend aligns with the characteristic behavior of scintillators, where the material's inherent properties significantly influence the generation and capture of photons, especially at higher energy levels.

The comparison of slopes between the two datasets implies that the more significant decrease observed in the experimental data may reflect a lower efficiency in collecting photons or converting energy at higher energy levels. The graph supports a comparison across different energy levels, providing quantitative insights into scintillator performance. As the Energy approaches 200 keV, the modeling and experimental data points align closely, indicating similar performance characteristics at lower energies.

This comparison provides a clearer perspective on the simulation performance of detectors, offering improved understanding compared to previous studies, and sheds light on the detection efficiency of other materials. Future research should focus on refining material models in simulations to more accurately represent the physical processes affecting scintillator performance. Additionally, expanding these studies to include a wider range of scintillator materials could provide a broader understanding of detector efficiencies for use in medical diagnostics, environmental monitoring, and nuclear safety.

Energy resolution and FWHM profile

In this section, the performance of the gamma detector is analyzed in terms of energy resolution and full width at half maximum (FWHM) at various photon energies. Figures 11(a) and 11(b) present the simulation and experimental results for FWHM and energy resolution profiles, respectively, as a function of photon energy in the current study. The results show that FWHM increases as the photon energy increases, indicating that the detectors may have limitations in energy resolution at lower energies. This is an important consideration in practical applications, as it highlights the need for clear differentiation of photon energy levels.

The energy resolution is calculated using FWHM and peak energy data. The results show the energy resolution of the plastic detector decreases as the photon energy increases, corresponding to an increase in FWHM. Overall, the detector demonstrates good performance in terms of energy resolution, which is also related to the energy absorption properties at lower energies. This suggests that radiation photons at higher energies are efficiently captured by the material, allowing the detector to provide a good response at those energy levels. The observed linear relationship indicates that, within the studied energy range, FWHM exhibits nearly proportionally with energy.

This pattern is common in scintillation detectors and can be explained by several factors. One key factor is the statistical characteristics of light production. As energy levels rise, the statistical variation in the number of light photons generated per interaction also increases, contributing to the broadening of energy distributions, as quantified by FWHM. In addition, the scintillator's inherent material properties influence this result. The response of the scintillator material to higher energies could lead to an increase in FWHM, with a greater efficiency of energy conversion to light at higher photon energies, resulting in broader peaks [32].

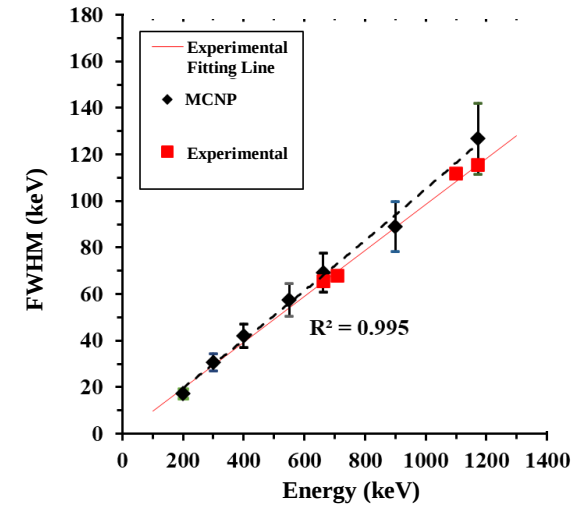

(a)

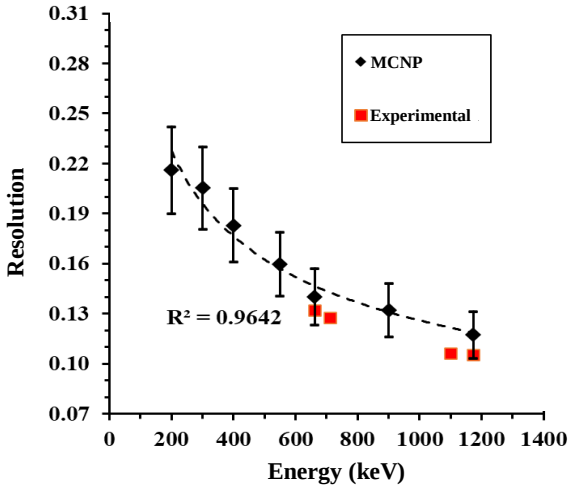

(b)

Fig. 11. Curve profile comparison of (a) FWHM; (b) Energy resolution.

Figure 11(b) represents the correlation between energy resolution and photon energy for a scintillation detector, observed through both simulations and experimental measurements. The graph indicates a noticeable correlation, where a rise in photon energy leads to a decrease in detector resolution, as reflected by the declining values on the y-axis, which denotes resolution. The trend is illustrated by a dashed line that fits the MCNP simulation data points, while the experimental data points are depicted for comparison. The fitting line demonstrates an inverse correlation between resolution and energy, indicating that the simulation model accurately captures the factors influencing detector performance across different energy levels. The MCNP simulation results demonstrate a gradual decrease in resolution as energy increases, concerning a non-linear pattern that is effectively represented by the employed fitting algorithm. The experimental data exhibits a consistent trend, though slightly elevated resolution values are observed at certain energies, such as approximately 600 keV and 1000 keV.

To enhance detector accuracy, simulation models need to be refined to better predict responses, especially concerning FWHM and energy resolution across varied photon energies. Investigating and developing new or improved scintillator materials could lead to advancements in energy resolution and reduced broadening at high energies. Furthermore, innovating detector designs that optimize the capture and conversion of high-energy photons will not only decrease FWHM but also elevate the overall performance of detectors, facilitating advancements in fields requiring exact radiation detection and analysis.

Potential application of validated model

The validated Monte Carlo model, designed to evaluate the performance of plastic scintillators, has broader applicability across various detector designs and radiation environments. For example, the model could be adapted to assess the efficacy of gamma-ray detectors used in nuclear facilities. Potential modifications might include optimizing the material composition of detectors to enhance their sensitivity and resolution for detecting specific isotopes commonly encountered in nuclear plants or waste management processes. Additionally, adapting the model to evaluate detectors in high-radiation environments such as nuclear reactors, could provide insights into improving the geometric design of detectors to minimize radiation damage and extend their operational life, thereby ensuring safety and efficiency in nuclear operations.

In the field of nuclear waste management, the validated Monte Carlo can be used to design optimized plastic scintillators, enhancing the monitoring and measurement of gamma radiation from stored waste materials. Plastic scintillators are

favored for their efficiency and cost-effectiveness, making them ideal for long-term monitoring setups where budget constraints and durability are key considerations. The model can simulate various storage configurations and shielding options, allowing for the calibration of scintillators to effectively detect specific gamma radiation signatures. This application ensures safety protocols, minimizes radiation exposure risks, and upholds regulatory standards, safeguarding both the environment and public health [33].

In airport security screening, the application of the Monte Carlo model can optimize the design and functionality of detectors used to identify and distinguish radioactive materials hidden in luggage or cargo. By simulating the interaction of gamma rays with various materials, the model helps develop detectors capable of accurately differentiating between harmless personal items and potential threats. This precision is important for maintaining high-security standards while ensuring the flow of passengers and goods is not unduly hindered, enhancing both safety and efficiency in high-traffic environments [34].

In the medical sector, specifically in cancer diagnosis and treatment, the application of the Monte Carlo model to optimize plastic scintillators for gamma-ray detection offers significant benefits. These scintillators are used to detect gamma rays emitted by radioactive tracers in both diagnostic imaging and therapeutic monitoring. By fine-tuning the scintillator design to maximize efficiency and resolution, the model enhances the accuracy of images, which is crucial for pinpointing the location and extent of cancerous growths or assessing the effectiveness of radiation therapy. The ability to simulate gamma-ray interactions with human tissue allows for the customization of detectors to patient-specific conditions, thereby improving the precision of treatments and diagnostics in oncology [35].

Building on this application, the validated model could be further extended to improve detector design and performance through strategic enhancements in material optimization and geometric configuration. To achieve this, a variety of additives with different compositions can be incorporated into plastic scintillators, each designed to serve a specific function. Nanoparticles like lead sulfide (PbS), gadolinium oxide (Gd_2O_3), or cerium oxide (CeO_2) can be added to enhance scintillation efficiency, boosting the material's ability to absorb gamma rays [36]. Primary dopants such as p-terphenyl or POPOP are used to adjust the wavelength of the emitted light to better match the photodetector's response [37]. This is complemented by secondary dopants like bis-MSB, which further shift the emission wavelength, enhance light yield, and accelerate the decay of scintillation light. Heavy metal compounds, including bismuth or lead-based additives, can be introduced to increase the detector's density and effective atomic number, thereby enhancing its photon interaction cross-section for higher energy photon detection [38].

Additionally, optical enhancers such as fluors or wavelength-shifting compounds can be employed to improve light transmission and reduce reabsorption, ensuring maximal light capture by the photodetector. Hybrid materials that combine plastic with inorganic scintillators also play a crucial role by using the high light yield of inorganic materials alongside the flexibility of plastics.

A practical example of optimizing geometric configuration in detector design involves comparing cylindrical versus flat geometries in portable radiation detectors. The Monte Carlo model simulates how radiation interacts with both cylindrical and flat-panel plastic scintillators under identical environmental conditions. Cylindrical detectors, offering 360-degree exposure, might excel in uniformly detecting ambient radiation from all directions, making them ideal for environmental monitoring or in-field nuclear waste management. In contrast, flat-panel detectors provide directional sensitivity, suitable for applications that require focused detection, such as conveyor belt setups in factory quality control or baggage scanning systems.

Building on this understanding, the upcoming research aims to further explore the model's potential applications by incorporating comparative studies that assess its performance against other established Monte Carlo simulation tools. These comparisons will highlight the specific advantages or unique capabilities of our model, such as its increased accuracy in predicting detector responses under varying radiation conditions or its enhanced computational efficiency. Through these comparative analyses, the study will not only affirm the strength of our model but also identify potential areas for further improvement in detector design. This approach provides a deeper understanding of how our model compares to recognized software like FLUKA or GEANT4, particularly in terms of user-friendliness, simulation speed, and the range of detectable energies.

Feasibility analysis of PPV as a scintillator

Poly(para-phenylene vinylene) (PPV) is a promising conjugated polymer that has not yet been thoroughly explored for gamma-ray detection application using Monte Carlo simulation.

The aromatic structure of PPV, consisting of repeating para-phenylene units, allows it to efficiently absorb energy from ionizing radiation. This aromatic framework supports effective energy transfer to light-emitting molecules (dopants) due to its long pi-conjugated system, enabling efficient electron delocalization and enhancing energy transfer efficiency during the scintillation process. Additionally, the presence of vinylene groups (-CH=CH-) in PPV further enhances its energy transfer capabilities, boosting the scintillation efficiency. The electronic resonance facilitated by the molecular structure of PPV plays a crucial role in the scintillation mechanism, ensuring the absorbed energy is effectively converted into light [39].

Furthermore, PPV exhibits excellent optical transparency, allowing the scintillation light to travel freely towards the detector with minimal absorption or scattering. This transparency facilitates the effective movement of photons to the detector, ensuring higher detection performance. Additionally, PPV's higher density (1.1–1.2 g/cm³) compared to PS (1.05–1.06 g/cm³) increases the number of interactions per unit volume, potentially leading to higher detection efficiencies. The material's excellent energy transfer capabilities and favorable optical properties further contribute to good resolution and sensitivity in gamma-ray detection, making PPV a potential alternative to traditional scintillator materials [40].

In this section, we simulate the response of the PPV detector using MCNP and compare it with the results of Polystyrene (PS) detectors. Figure 12(a) represents the pulse height distributions for both materials, PPV (red line) and PS (blue line), as a function of energy (in keV), providing insight into their scintillation detection characteristics. Both PPV and PS exhibit clear peaks, with the maximum counts at approximately 490 keV. Notably, the PPV detector shows a slightly higher peak than the PS detector, suggesting potentially stronger interaction with gamma rays, and consequently, a higher count rate at peak energy. Furthermore, the PPV peak appears sharper and narrower compared to PS, indicating better energy resolution. This sharper peak suggests that PPV may be more effective in differentiating between similar energy levels, making it a promising material for application.

In Fig. 12(a), PS and PPV curves show high counts at lower energy levels, which is due to the Barium (Ba) X-ray peak at approximately 32 keV, which is a result of the decay process of the ^{137}Cs atom [41]. As energy increases, both materials exhibit an increase in counts approaching the peak energy, followed by a gradual decline. However, PPV displays a clearer signal with a more defined peak and less spread in the tail compared to PS. This sharper signal is advantageous because it reduces the likelihood of overlap from multiple sources and minimizes error in peak detection, contributing to improved accuracy in distinguishing different energy levels.

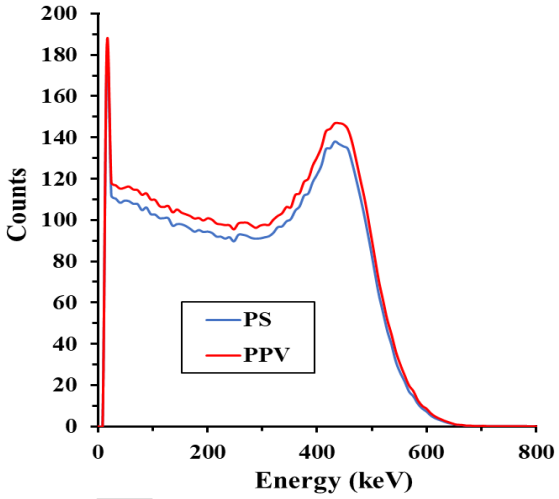

(a)

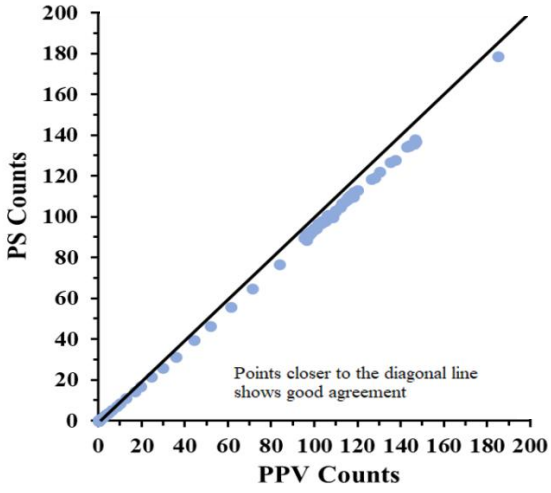

(b)

Fig. 12. Comparison of detector responses for PPV vs. PS: (a) Pulse height distributions under gamma-ray irradiation; (b) Counts at various energy levels.

Figure 12(b) compares the count rates between PPV and PS as derived from simulation data. The diagonal line in the graph represents a benchmark at which the count rates of PPV and PS would be equivalent. Data points that lie near this line indicate similar performance between the two materials under the same conditions. Most data points are clustered near the diagonal, suggesting that for most tested energy levels or scenarios, PPV and PS exhibit comparable count rates. This proximity to the diagonal further highlights the

similar performance capabilities of both scintillators under the conditions tested.

The data points spread around the diagonal line, with a tendency to cluster slightly above or directly on the line, especially in the mid to high counts range (60 to 200 counts). This pattern suggests that PPV occasionally registers slightly higher counts than PS, or it may reflect a variation in sensitivity or efficiency between the two materials at certain energy levels. In the lower count range (0-60 counts), the points are tightly aligned along the diagonal, indicating very similar responses from both materials when detecting lower levels of radiation. However, at the higher count levels, the data points show a slight divergence from the diagonal line. While still relatively close, this suggests that there are subtle differences in how each material responds to higher radiation levels. It appears that PS may have a slight edge in detection efficiency or energy resolution at these higher counts, which could be attributed to PS's well-established properties in scintillation and energy resolution.

While PPV exhibits good characteristics as a scintillator, several limitations make it less advantageous compared to Polystyrene (PS). The complex synthesis process of PPV, along with the specific requirements for material processing, results in higher production costs compared to PS. PPV production often involves specialized polymerization stages and the use of expensive chemicals, thereby increasing the overall cost [42]. Additionally, one of the significant challenges faced by PPV is the degradation of its chemical structure when exposed to radiation over extended periods. As a relatively new material in scintillator applications, PPV has not yet achieved the same level of popularity as PS within the industry. This limited adoption has resulted in underdeveloped standards for its use in radiation detection applications, and its implementation remains scarce [43]. Furthermore, there is a notable lack of research focused on optimizing PPV specifically for scintillator applications compared to PS. Most existing studies primarily address the fundamental properties of PPV rather than its specific performance as a scintillator, leading to a lack of comprehensive data necessary for performance optimization.

CONCLUSION

In this study, we developed a methodology for simulating a plastic detector using the MCNP code, complemented by experimental work to assess detector performance in detecting gamma sources ranging from 100 keV to 1300 keV. The experimental results were then compared with the simulation data. Both experimental and simulated data contributed to generating curves that, when compared, displayed a satisfactory alignment. Notably, a deviation of 8.04 % was observed at 662 keV for ^{137}Cs.

The study successfully developed a validated simulation model that demonstrates good alignment with the experimental results, effectively addressing the efficiency challenges faced by current plastic detectors. This work not only confirms the efficacy of simulation in enhancing detector development but also reduces costs and improves the credibility of simulation models. These results demonstrate the Monte Carlo code as a reliable, robust, and efficient tool for estimating detector performance.

The potential upcoming research may explore the applications of our model by incorporating comparative studies that assess its performance against established Monte Carlo simulation tools like FLUKA and GEANT4 [44,45]. These studies aim to highlight our model's advantages, including its increased accuracy in predicting detector responses under varied radiation conditions and enhanced computational efficiency.

ACKNOWLEDGMENT

The authors wish to acknowledge the National Research and Innovation Agency (BRIN) for providing research tools and materials. Appreciation is also extended to all individuals and parties who have lent their assistance to this endeavor. The collective effort, whether through discussion, provision of sources, or general support, has played a pivotal role in the successful completion of this work.

AUTHOR CONTRIBUTION

G. E. Putro – Conceptualization, Methodology, Data Collection, Analysis and Visualization, Writing Original Draft, Review & Editing, Draft Final Revision, M. R. Omar – Supervision, Conceptualization, Writing Review & Critical Revision, Kasmudin – Conceptualization, Writing Review & Critical Revision, Supervision, H. L. Nuri – Conceptualization, Data Collection and Field Experimentation, M. Pancoko – Data Collection and Field Experimentation, A. Jami – Data Collection and Field Experimentation, H. Subhiyah – Data Collection and Field Experimentation.

REFERENCES

1. V. Vaněček, J. Páterek, R. Král *et al.*, J. Cryst. Growth **573** (2021) 126307.
2. G. L. Montagnani, L. Buonanno, D. Di Vita *et al.*, Nucl. Instrum. Methods Phys. Res. A **931** (2019) 158.
3. S. O'Neal, N. J. Cherepy, S. Hok *et al.*, *High-Light Yield Bismuth-Loaded Plastic Scintillators*, Proceedings Hard X-Ray, Gamma-Ray, and Neutron Detector Physics XXIII, **11838** (2019) 12.
4. W. Chaiphaksa, P. Borisut, J. Kaewkhao *et al.*, Integ. Ferroelectrics **239** (2023) 71.
5. S. Kilby, Z. Jin, A. Avachat *et al.*, J. Radioanal. Nucl. Chem. **320** (2019) 37.
6. S. S. Chirayath, C. R. Schafer, G. R. Long, Ann. Nucl. Energy **151** (2021) 107911.
7. G. Trabidou, I. E. Stamatelatos, P. Kritidis *et al.*, *Evaluation of External Doses from Exposure to Gamma Sources in the Soil Using the MCNP Code*, Proceedings HNPS Advances in Nuclear Physics, **10** (2019) 203.
8. S. Yani, R. Tursinah, M. F. Rhani *et al.*, J. Phys. Conf. Ser. **1127** (2019) 012014.
9. J. A. Kulesza, T. R. Adams, J. C. Armstrong *et al.*, MCNP Theory & User Manual LA-UR-22-30006, Code Version 6.3.0, 1st ed. (2022).
10. C. Holroyd, M. Aspinall, T. Deakin, EPJ Web Conf. **253** (2021) 11002.
11. B. T. Koo, H. C. Lee, W. G. Shin *et al*, J. Instrum. **14** (2019) P12015.
12. R. Ricci, T. Kostou, K. Chatzipapas *et al*, Cryst. **9** (2019) 398.
13. I. Mouhti, A. Elanique, M.Y. Messous *et al.*, J. Radiat. Res. Appl. Sci. **11** (2018) 335.
14. A. Kamiya, M. Goto, T. Kodama *et al.*, Photomultiplier Tubes Basics and Applications, 4th ed., Hamamatsu Photonics, Shizuoka (2017) 25.
15. E. Asano, D. Coleman, G. Davidson *et al.*, Nucl. Instrum. Methods Phys. Res. A, **1031** (2022) 166568.
16. A. S. Roy, K. Banerjee, P. Roy *et al.*, J. Instrum. **16** (2021) P07045.
17. H. S. Bush, M. H. Eisa, A. Ramizy *et al.*, J. Optoelec. Biomed. Mat. **12** (2020) 101.
18. J. Ryu, J.-Y Park, H.-W. Lee *et al.*, J. Radioanal. Nucl. Chem. **329** (2021) 959.
19. S. Buakham, S. Sangaroon, K. Ogawa *et al.*, J. Phys. Conf. Ser. **2431** (2023) 012070.
20. M. I. Abbas, M. S. Badawi, A. A. Thabet *et al.*, Appl. Rad. Isot. **163** (2020) 109139.
21. A. Sato, A. Magi, M. Koshimizu *et al.*, RSC Adv. **11** (2021) 15581.
22. A. Yüksel, M. Tombakoğlu, Appl. Rad. Isot. **166** (2020) 109333.
23. M. J. Kumwenda, Tanzania J. Eng. Tech. **39** (2020) 104.
24. J. Gil Rostra, K. Soler-Carracedo, L. L. Martín, *et al.*, Dyes Pigm. **182** (2020) 108625.
25. Y. Tang, S. Cabrini, J. Nie *et al.*, Chin. Chem. Lett. **31** (2020) 256.
26. D. Serraïma-López, M. Guillén, H. Bagán *et al.*, Appl. Radiat. Isot. **211** (2024) 111409.
27. G. Z. Woźniak and B. Kozłowska, Pol. J. Med. Phys. Eng. **29** (2023) 92.
28. G. Paternò, P. Cardarelli, M. Gambaccini *et al.*, Phys. Med. Biol. **65** (2020) 245002.
29. Junios, F. Haryanto, Z. Su'ud *et al.*, J. Phys. Conf. Ser. **1493** (2020) 012012.
30. Y. Tariwong, H. J. Kim, N. D. Quang *et al.*, Radiat. Phys. Chem. **226** (2024) 112241.
31. C. M. Salgado, L. E. B. Brandão, R. Schirru, *et al.*, Prog. Nucl. Energy **59** (2012) 19.
32. O. Smirnov, J. Instrum. **18** (2023) P10026.
33. G. Haquin, H. Zafrir, D. Ilzycer *et al.*, J. Environ. Radioact. **237** (2021) 106693.
34. L. Marques, L. Félix, G. Cruz *et al.*, Sens. **23** (2022) 329.
35. X. Sun, H. Wang, X. Li *et al.*, Future Gener. Comput. Syst. **102** (2020) 978.
36. M. Mazhdi, M. J. Tafreshi, Nucl Instrum Methods Phys Res A, **959** (2020) 163604.
37. D. M. Niedzwiedzki, D. Mulrow, L. G. Sobotka, J. Phys. Chem. A, **126** (2022) 5273.
38. H. A. El Batal, F. H. El Batal, M. A. Azooz *et al.*, J. Non-Cryst. Solids, **572** (2021) 121090.
39. F. L. de O. Paula, L. L. e Castro, L. A. R. Junior *et al.*, Sci. Rep. **9** (2019) 18131.
40. S. A. A. Fuzi, M. H. Hj. Jumali, B. A. Al-Asbahi *et al.*, Thin Solid Films **683** (2019) 90.
41. T. Yanagida, M. Sakairi, T. Kato *et al.*, Appl. Phys. Express **13** (2020) 016001.

42. D. Becker, B. P. Biswal, P. Kaleńczuk *et al.*, Chem. Eur. J. Chemistry, **25** (2019) 6562.

43. Z. Lin, S. Lv, Z. Yang, J. Qiu *et al.*, Adv. Sci. **9** (2022) 2102439.

44. P. H. Lam, P. T. Dung and P. Q. Trung, Atom Indones. **50** (2024) 221.

45. B. El Azzaoui, O. Kabach, R. Outayad *et al*., Atom Indones. **50** (2024) 231.